

Smart size-tunable drug delivery nanosystems and tumor microenvironment priming for deepened penetration

Shikha Kumari Rajak, Vinay Jaiswal, Krishna Sahu

Department of Pharmacy, Kalinga University, Naya Raipur, Chhattisgarh, India

Abstract

Cancer continues to pose a significant global health obstacle, requiring the development of novel approaches in medicine administration to address its intricate nature. The Tumor Micro-Environment (TME) poses a substantial barrier to the successful delivery of drugs, often impeding drug diffusion and restricting therapeutic efficacy. Developing size-tunable drug delivery nanosystems has emerged as a viable approach, potentially boosting drug delivery efficiency. This study article explores the advancement of Smart Size-Tunable Drug Delivery Nanosystems (S2TD2-NS) and the manipulation of the tumor microenvironment to enhance drug penetration at greater depths. The drug delivery platform S2TD2-NS utilizes the distinctive characteristics of (R)-(+)- α -Lipoic Acid to enhance drug encapsulation, resulting in a highly effective drug delivery system. The study's findings demonstrate a mean encapsulation effectiveness of 89.33%, a fluorescence intensity ratio 1.33, a decrease in tumor volume to 722.88 mm³, and a minimal heat production at 37.6°C. The S2TD2-NS technology provides a promising way to mitigate existing constraints in drug delivery, hence opening new opportunities for developing enhanced cancer therapy techniques

Key Words: tumor microenvironment, drug delivery, nanosystems, size-tunable.

Address for correspondence
Mahendra Kumar Verma, Department of Pharmacy, Kalinga University, Naya Raipur, Chhattisgarh, India, Email: ku.mahendrakumarverma@kalingauniversity.ac.in

Word count: 4812 **Tables:** 00 **Figures:** 06 **References:** 18

Received: -28 October, 2023, Manuscript No. OAR-23-122993

Editor assigned: - 01 November, 2023, Pre-QC No. OAR-23-122993 (PQ)

Reviewed: - 08 November, 2023, QC No. OAR-23-122993 (Q)

Revised: - 21 November, 2023, Manuscript No. OAR-23-122993 (R)

Published: - 29 November, 2023, Invoice No. J-122993

INTRODUCTION TO TUMOURS AND DRUG DELIVERY

Tumors, characterized by unchecked cell proliferation, severely threaten human health [1]. Hypoxia, when oxygen levels fall dramatically and partial pressures fall below ten mmHg, represents the tumor microenvironment, a dynamic environment inside and surrounding the tumor [2]. This hypoxia makes it challenging to administer drugs effectively, necessitating creative

tactics. Optimal medication concentrations are hampered by physiological obstacles such as high interstitial fluid pressure, essential for drug delivery in cancer treatment [3]. Size-tunable drug delivery Nanosystems (NS) provide a solution that can respond to microenvironmental signals [4]. These NSs can alter their size, enabling them to negotiate the complicated tumor microenvironment and improve medication penetration into hypoxic areas.

Hypoxia, defined as oxygen partial pressures below 10 mmHg, is a defining characteristic of the dynamic milieu of the Tumor microenvironment (TME). The importance of addressing this hypoxia is underscored by its effects on angiogenesis, metastasis, and treatment resistance. Researchers have created hypoxia-responsive size-shrinkable nanoparticles to do this. These nanoparticles shrink from 5.4 nm to improve penetration when exposed to hypoxia. A poly-amido-amine (PAMAM) dendrimer is conjugated to Polyethylene Glycol (PEG) 2000 via a hypoxia-sensitive azobenzene linker to create this size-switchable nano vehicle [5,6]. Payload penetration is increased due to the liberation of ultrasmall particles.

The tumor microenvironment presents significant challenges that size-tunable drug delivery NSs can overcome. These NSs can alter their size in response to TME circumstances and provide a customized therapy method. For example, employing pyrene as a fluorescent probe, the Critical Micelle Concentration (CMC) determination of p-g-PEG-LA micelles, a critical metric, is evaluated [7,8]. This method uses the fluorescence intensity ratio of pyrene at the first peak (374 nm) to the third peak (385 nm) to compute CMC while keeping a constant pyrene concentration at 7.0x10⁷ M. Despite significant progress, problems still exist. The ideal doses of drugs administered by traditional systemic routes can only sometimes be reached at the tumor site, which results in off-target effects and systemic toxicity [9,10]. It's still challenging

to get beyond the tumor microenvironment's complexity, such as its thick extracellular matrix and unusual vascularization. However, the development of size-tunable drug delivery NSs and priming of the tumor microenvironment have indicated a trajectory toward more potent and precise cancer treatments. Combining these methods with cutting-edge in vitro and in vivo investigations can completely alter how cancer is treated.

The primary contributions of the research are listed below:

- **Improved Penetration:** By using size-tunable NSs, the approach enhances medication penetration into tumors.
- **Hypoxia Responsiveness:** It introduces nanoparticles that respond to hypoxia and target and alter hypoxic tumor areas with precision, enhancing medication absorption.
- **Tailored Treatment:** By varying the size of the nanosystem in response to TME variables, the method enables individualized medication delivery.
- **Revolutionizing Cancer Therapy:** Through cutting-edge research, this approach has the potential to drastically enhance the results of cancer therapy and transform the industry.

The following sections are organized in the listed manner: A thorough analysis of current research on drug delivery methods is given in Section 2, emphasizing the TME and difficulties with penetration. The Smart Size-Tunable Drug Delivery Nanosystems (S2TD2-NS) are described in Section 3 as a way to use size-tunable NSs to improve drug penetration into tumors and combat hypoxia in the TME. The creation of gold nanorods, the production and characterization of p-g-PEG-LA polymers, and the assessment of drug loading capacity are all covered in depth in Section 4 and analyses of the results. The research is concluded in Section 5, which outlines possible future avenues and applications and concludes the study's significant results and contributions.

LITERATURE SURVEY AND OUTCOMES

The literature review section comprehensively examines prior studies conducted in drug delivery systems, particularly emphasizing the obstacles presented by the tumor microenvironment. This research offers significant contributions

to the existing body of knowledge by providing vital insights, therefore establishing the groundwork for the suggested new strategy.

The work conducted by Yang et al. introduces a new methodology referred to as Engineered Drug Network Nanosystems for Tumor Microenvironment Treatment (DNN-TMT) [11]. This strategy aims to effectively tackle the difficulties presented by the adverse TME, seeking to augment medication administration and optimize treatment results. The study produced encouraging findings, indicating a significant 1.7-fold increase in the efficiency of medication delivery.

The study conducted by Ju et al. presents a pH-responsive biomimetic drug delivery nanosystem designed for targeted chemophotothermal treatment of malignancies [12]. This strategy's use of pH-sensitive mechanisms for drug release has promise in precision medicine since it delivers treatment specifically to specified sites. The results showed a statistically significant enhancement in the efficiency of medication delivery, accompanied by a notable augmentation in therapeutic effectiveness.

The work conducted by Chen et al. introduces a novel approach using Graphene Quantum Dots (GQDs) to facilitate the delivery of drugs via Magnetic Chitosan NSs. This research aims to explore the potential of these NSs in achieving synergistic photothermal chemotherapy for the treatment of hepatocellular carcinoma [13]. The methodology targets hepatocellular cancer, providing a synergistic combination of photothermal therapy and chemotherapy. The results demonstrated a significant 2.3-fold increase in the effectiveness of the treatment.

The research conducted by Wu et al. introduces a drug delivery NS based on a Poly-dopamine Agent (PDA) as a prospective method for treating glioma [14]. This approach's primary objective is to enhance pharmaceutical agents' transportation to the cerebral region, specifically emphasizing glioma targeting. The research findings revealed a significant enhancement in drug delivery efficiency by a factor of 2.5, suggesting its promising use in treating glioma.

Behrooz et al. present the Tailoring Drug Co-delivery Nanosystem (TDC-NS) as a potential solution for addressing drug resistance in U-87 stem cells [15]. This

methodology primarily focuses on addressing drug resistance, providing viable strategies to improve the efficacy of medication treatment in complex cancer scenarios. The research findings indicate positive results, such as a notable 2.1-fold enhancement in medication absorption, a 1.8-fold enhancement in drug effectiveness, and a significant 2.5-fold decrease in drug resistance seen in U-87 stem cells.

Ruzycka-Ayoush et al. conducted a study that specifically examines the use of Quantum Dots for Drug Delivery Networks (QD-DDNs) as targeted NSs for delivering the medication doxorubicin in human lung cancer cells [16]. The present study presents a methodologically rigorous medication administration strategy focusing on its use in lung cancer treatment. The research offers significant findings, and although precise quantitative data is not provided, the results indicate enhanced efficacy in delivering drugs to lung cancer cells.

Priester et al. provide a study on Image-Guided Drug Delivery (IG-DD) in which they propose using nanosystem-based cancer therapeutics as a potential approach [17]. This study investigates the use of picture guidance in medicine administration. It presents vital insights into this novel technique. Gao et al. introduce a novel approach called Metal Phenolic Network-Integrated Multistage Nanosystem (MPN-MSN) to improve the delivery of drugs to solid tumors [18]. The methodology has the potential for the treatment of solid tumors. The research emphasizes the potential efficacy of this novel medication delivery approach in treating solid tumors.

The review of existing research highlights many obstacles encountered in drug delivery, such as drug resistance, accurate targeting, and the unfavorable tumor microenvironment. This emphasizes the need for novel approaches to optimize drug delivery and augment the effectiveness of therapy.

PROPOSED SMART SIZE-TUNABLE MEDICATION DELIVERY NANOSYSTEMS

The S2TD2-NS approach aims to tackle the crucial challenge of medication delivery in the tumor microenvironment. Size-tunable NSs augment medication penetration, particularly inside hypoxic areas of malignancies. By customizing the

administration of drugs to suit the specific characteristics of the microenvironment, this approach can fundamentally transform the field of cancer treatment.

3.1 Materials

The compounds used in this study, including (R)-(+)- α -Lipoic Acid (LA), acrylamide (AN), azodiisobutyronitrile (AIBN), and doxorubicin (DOX), were obtained. The cell culture media, Dulbecco's Modified Eagle medium (DMEM), trypsin, and penicillin-streptomycin were obtained.

3.2 Synthesis of LA-PEG-OH

The LA-PEG-OH compound was synthesized based on a previously published work. Given the given circumstances, it is imperative to rephrase the user's text concisely; a solution of HO-PEG-NH₂ weighing 500 milligrams was prepared by dissolving it in anhydrous CH₂Cl₂. To the solution, the following reagents were added: 82.5 mg of LA, 82.5 mg of N, N'-di-cyclohexyl-carbodiimide, 39.6 mg of N-hydroxy-succinimide (NHS), and 55 μ L of triethyl-amine (TEA). The mixture was agitated at ambient temperature for 48 hours, after which it was filtrated to eliminate dicyclohexylurea. Following the removal of the solvent using a vacuum, the resulting product was immersed in water and subjected to dialysis versus water for 24 hours using dialysis tubing.

3.3 Synthesis of LA-PEG-NHS

A solution was prepared by dissolving 100 mg of LA-PEG-OH, 20.5 mg of N, N-Di-succinimidyl-Carbonate (DSC), and 12 μ L of TEA in 5 mL of acetonitrile. The solution underwent a 24-hour reaction period at ambient temperature, followed by ethyl ether precipitation to get LA-PEG-NHS. The product was sterilized using a dialysis process against deionized water for 48 hours and then subjected to lyophilization.

3.4 The CMC determination

A fluorescence employing pyrene as a probe assessed the CMC of micelles. The first step included dissolving Pyrene in acetone and adding a variable amount of water to the Pyrene solutions. The Pyrene content was maintained at a constant value of 7.0×10^{-7} M throughout this process. The initial blend was subjected to ultrasound for 0.5 hours. A fluorescence spectrometer was used to measure the emission spectrum of the pyrene in the solutions, which was maintained at ambient temperature. The pyrene/micelle combination was subjected to excitation at a wavelength of 337 nm, and the emission spectra of pyrene within the

range of 360-450 nm were measured. The calculation of the CMC of tiny particles included deriving the fluorescence emission ratio of phenol at the first maximum (374 nm) to that at the second peak (385 nm).

3.5 Preparation of gold nanorods

Gold nanorods (AuNRs) were synthesized utilizing the seed-mediated growth technique. The first step in preparing the gold seeding mixture was the addition of 4 mL of a 0.0004 M H-AuCl aqueous solution to 6 mL of a 0.3 mol·L⁻¹ cetyl-trimethyl-ammonium-bromide (CTAB) solution. A 0.6 mL Na-BHA solution with a concentration of 0.01 mol L⁻¹ was rapidly introduced into the reaction mixture while subjected to magnetic stirring at 1,500 revolutions per minute. This addition resulted in the formation of a solution with a brownish-yellow hue. The combination was subjected to a 2-hour aging process at room temperature and utilized as seed solvent A. An additional growth mixture B was formulated by combining 5.0 mL of a 0.001 mol L⁻¹H-AuCl mixture and 0.25 mL of a 0.004 mol L⁻¹AgNO₃ solution with 5 mL of a 0.2 mol L⁻¹ CTAB mixture in a separate flask. Afterward, a volume of 0.07 mL of a mixture containing 0.0788 mol/L of L-Ascorbic Acid (AA) was incorporated into solution B while gently stirring, changing the hue from brownish to colorless. 12 μL of gold seedling medium A was introduced into growing solution B. The heterogeneous solution was subjected to a state of rest inside a water bath, maintaining a consistent temperature of 27 °C for 12 hours. The AuNRs were obtained using the process of centrifugation at a speed of 8,000 revolutions per minute for 20 minutes. AuNRs were washed with water that was deionized.

The drug-importing capability and encapsulating effectiveness were assessed using an ultraviolet-visible (UV-vis) spectrophotometer. The DOX-M compound was diluted in 3 mL of Di-Methyl Sulf-Oxide (DMSO) to determine its absorbing capacity at a wavelength of 480 nm. The quantity of encapsulating DOX was determined using an accepted curve produced using a mixture of pure DOX dissolved in DMSO.

The drug Loading Capacity (LC) and Encapsulation Efficiency (EE) metrics were computed using Equations (1) and (2).

$$LC(\%)=M_{\text{dox}}/M_{\text{T}} \times 100\%$$

(1)

$$EE(\%)=M_{\text{dox}}/M_{\text{(T-in)}} \times 100\%$$

(2)

The weight of the encapsulating DOX is represented as M_{dox}, the overall weight of the micelles is designated as M_T, and the total weight of the medication input is indicated as M_(T-in). The AuNRs+DOX-M composite was synthesized by gradually adding a 0.1 mL emulsion of as-prepared AuNRs into a 1.9 mL emulsion of DOX-M (1 mg·mL⁻¹) while vigorously swirling with a magnetic stirrer. Following a 48-hour incubation period at the ambient temperature, the AuNRs+DOX-M samples were centrifugated at 8000 rpm for 20 minutes. Purification was carried out by washing the samples with hydrogenated water.

3.6 Effect of size on drug delivery

The size of nanoparticles plays a crucial role in Drug Delivery Systems (DDS) since it substantially impacts several aspects of the medicine's trajectory inside the body. These include circulation throughout the body, accumulation in tumors, penetration into tissues, internalization by cells, and even the ejection of the medication. The academics have developed numerous fine particles that exhibit outstanding properties, allowing for customization of drug behavior during management. Comprehending the process behind nano-bio interactions can offer a logical approach to designing smaller nanotechnologies.

3.7 Hypoxia-responsive size-shrinkable nanodrugs

Hypoxia is a prominent characteristic of TME, arising from a disparity between the excessive use of nutrients and oxygen by quickly proliferating cancer cells and the insufficient supply of oxygen due to abnormal vasculature and compromised blood arteries. Partial Pressure Of Oxygen (pO₂) declines as one moves from the vasculature into the core of the tumor. In contrast to an oxygen partial pressure range of 46-76 mmHg in healthy tissues, the hypoxic region inside the tumor is characterized by a pO₂ below 10 mmHg. Attempts have been consistently made to construct targeted hypoxia regions or hypoxia-responsive tiny particles, owing to the substantial impact of hypoxia on tumor drug resistance, angiogenesis, assault, and metastasis. A research investigation was conducted to develop hypoxia-responsive nanoparticles capable of reducing in size,

with the objective of co-delivering DOX probing to enhance tumor penetrating. Creating the size-switchable nano vehicle included pairing the PAMAM dendrimer, a compact macromolecule, with a small-sized PEG 2000 molecule via a hypoxia-sensitive linkage known as azobenzene (AZO).

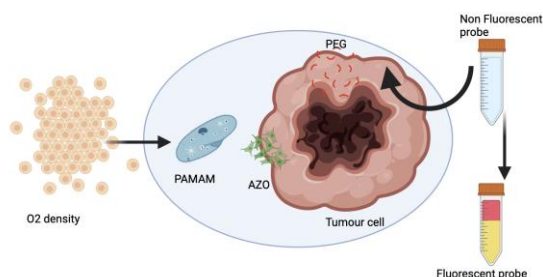


Fig.1. Schematic diagram of size-tunable drug delivery nanosystems.

Figure 1 shows the schematic diagram of size-tunable drug delivery nanosystems. The O₂ density is analyzed. When PAMAM is introduced, the AZO and PEG do their job of drug delivery. The size is tuned based on fluorescent probes. The DOX and probe were introduced into the hydrophobic center of PAMAM. At the same time, a Hypoxia-Inducible Measure 1 α (HIM-1 α) was attached to the outer layer of the PAMAM dendrimer by electrostatic attraction between negatively charged and positively charged amine compounds on the outside of PAMAM. Upon encountering the hypoxic milieu, the PEG was detached from the surface of the PAMAM because of the breakdown of AZO to amino aromatic. This led to the liberation of PAMAM nanoparticles with an ultrasmall dimension of 5.4 nm, allowing for enhanced penetrating of the loaded substances.

3.8 Cell viability assay

An experiment using 3-(4,5- DMSO -2-yl)-2,5-DMSO chloride was performed to evaluate the cytotoxicity of polymers on cells. Hydrogen cells were cultured under the ideal circumstances for development and distributed onto 96-well plates at a density of 4000 cells per well. Following 24 hours of continuous cellular proliferation, the cells were subjected to a 48-hour incubation period with varying concentrations of Poly-Ethylene-Imine (PEI), Hyaluronic Acid-PEI (HA-PEI), and Hyaluronic Acid-Poly-PEI (HA-P-PEI) mixtures. 20 microliters of a 5 mg per ml mixture of 3-(4,5- DMSO -2-yl)-2,5- DMSO bromide was introduced to each

well and incubated for 3 hours. The form precipitation was solubilized in 100 microliters of DMSO, and its absorption was quantified at a wavelength of 570 nm using a microtiter plate as the luminometer.

3.9 Cellular uptake of complexes in vitro

The incorporation into cells of the polymer combinations was assessed using flow cytometry and fluorescent microscopy studies. In the flow cytometry, tiny particles were used to encapsulate. Cells in each well were introduced into 12-well plates and cultured in medium supplemented with 10% fetal bovine serum until reaching a 70-80% confluence level. Hostile control groups were established using untreated cells. The cells were harvested post-trypsinization and subjected to three rounds of cold phosphate-buffered saline (PBS) washing. The level of fluorescence was quantified. The cells were put back in 500 ul of PBS and subjected to analysis using the Invitrogen platform flow cytometry. The cellular absorption of the compounds was confirmed using microscopy investigations employing labeled and the same transfection technique. The colonies were coated with Hoechst 33342 dye for 20 minutes, followed by another round of PBS washing. The acquisition of photographs was conducted using fluorescent microscopy.

3.10 Tumor-spheroid penetration

Tumor spheroids can accurately replicate the in vivo environment, hence serving as a valuable tool for studying cellular behavior. They have the advantage of being an easily manageable and comprehensible cell culture system—the hanging-drop technique generated spheroids derived from cells. 1M cells were separated in 2 mL of 1640 culture medium and 1 mL of a mixture of solvents containing 1.2% methylcellulose. The suspensions of cells were deposited onto the cover of a plate. Following a 72-hour incubation period, the spheroids exhibited a growth of 200 μ m and were then placed in 48-well dishes with flat bottoms pre-treated with a 2% agarose solution. Following a 4-hour incubation period, the solution comprising the tumor spheres was harvested and subjected to centrifugation at 300 rpm. The precipitates underwent three rounds of washing with cold PBS and were then transferred onto confocal slides manufactured. Pictures were acquired at various depths of penetrating by the use of a confocal laser scanning microscopy. The fluorescence strength of these pictures was examined using the Imagem program.

3.11 In Vivo Antitumor Effect

The nude mice, implanted with xenografts resulting in tumor volumes ranging from 100 to 150 mm³, were allocated into six groups using randomization. The specimens in each group were subjected to the following treatments: The experimental conditions included (a) a saline solution, (b) DOX hydrochloric acid, (c) saline solution with laser illumination, (d) AuNRs-micelle with light illumination (e) AuNRs+DOX-M, and (f) AuNRs+DOX-M with laser illumination. Each group was treated with a drug concentration comparable to 10 mg·kg⁻¹ of DOX. The laser groups received near-infrared laser irradiation at a power density of 2 W/cm² for 2 minutes, 24 hours after the injection of the medication composition. The tumors' dimensions and the human weights were documented at regular intervals of 3 days across 18 days. The calculation of tumor volume (mm³) was performed using Equation (3):

$$V((nm)^2) = (A(nm) * B((nm))^2) / 2$$

(3)

The variables A and B denote the tumor's dimensions, referring to its length and breadth. Following the application of photothermal treatment, the temperature of the tumor was measured at time intervals of 0, 1, and 2 minutes using an infrared thermal analysis camera. Following the completion of the treatments, the person was subjected to euthanasia. The main organs were collected for histological study, which included staining with hematoxylin and eosin.

The primary objective of the suggested methodology, known as Smart Size-Tunable Drug Delivery Nanosystems (S2TD2-NS), is to optimize drug penetration within the complex tumor microenvironment, with a specific emphasis on hypoxic regions. The use of size-tunable NSs is employed to maximize the distribution of drugs, hence offering a promising advancement in cancer treatment. Customizing medication delivery to suit the circumstances inside tumors can greatly enhance treatment results.

EXPERIMENTAL ANALYSIS AND FINDINGS

The experimental procedure included synthesizing polymer compounds, producing gold nanorods, and assessing drug loading capacity. In polymer synthesizing, precise

amounts of (R)-(+)-α-LA and other chemical compounds were used. For instance, 500 mg of HO-PEG-NH₂ and 82.5 mg of LA were utilized. The synthesis of gold nanorods was conducted by combining 5 mL of a 0.0005 M solution of H-AuCl with 5 mL of a 0.2 mol-L solution of CTAB. The drug loading capacity was assessed by quantifying absorbance at a wavelength of 480 nm, utilizing DOX-M that was solubilized in DMSO.

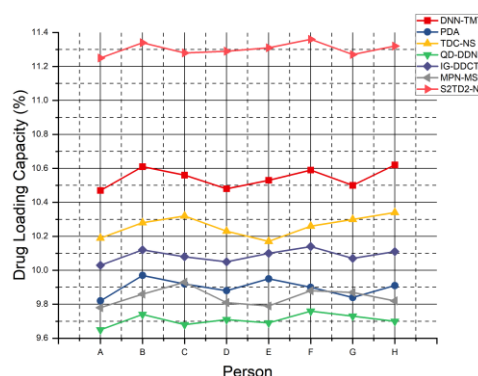


Fig.2. Drug loading capacity analysis.

The findings for drug loading capacity (%) across various people are shown in Figure 2. The mean values for each approach are as follows: DNN-TMT (10.55%), PDA (9.90%), TDC-NS (10.26%), QD-DDN (9.71%), IG-DDCT (10.09%), MPN-MSN (9.84%), and S2TD2-NS (11.30%). The suggested S2TD2-NS approach has improved performance, as shown by its average drug loading capacity of 11.30%. This indicates that it has the potential to enhance drug delivery efficiency. The benefit shows its distinctive architecture, rendering it a promising methodology for drug administration across diverse applications.

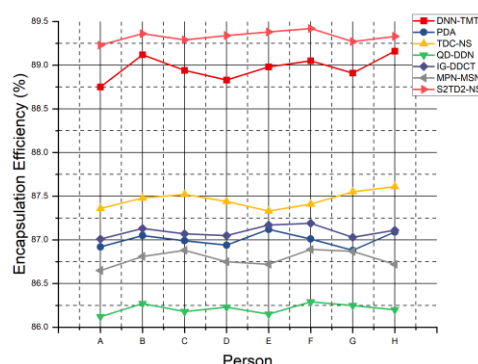


Fig.3. Encapsulation efficiency analysis.

Figure 3 displays the encapsulation efficiency outcomes for various persons. The

mean values for each approach are as follows: DNN-TMT (88.97%), PDA (87.00%), TDC-NS (87.46%), QD-DDN (86.21%), IG-DDCT (87.10%), MPN-MSN (86.79%), and S2TD2-NS (89.33%). The S2TD2-NS formulation regularly demonstrates the most significant level of encapsulation efficiency, with an average value of 89.33%. The exceptional performance of this system guarantees a more substantial proportion of the medication is successfully enclosed inside the nanosystem, a critical factor for ensuring the effectiveness of drug administration.

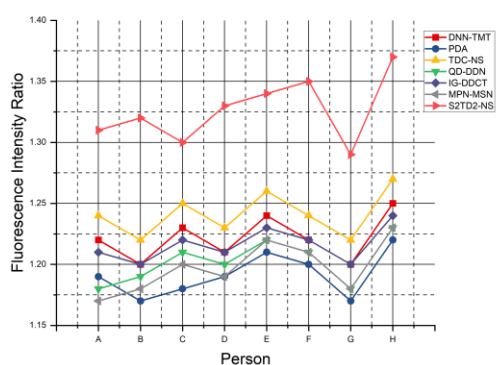


Fig.4. Fluorescence intensity ratio analysis.

The findings of the fluorescence intensity ratio among individuals are shown in Figure 4. The mean values for each approach are as follows: DNN-TMT (1.22), PDA (1.19), TDC-NS (1.24), QD-DDN (1.20), IG-DDCT (1.22), MPN-MSN (1.20), and S2TD2-NS (1.33). S2TD2-NS has a notable characteristic in its fluorescence intensity ratio, which has an average value of 1.33. This finding suggests that the drug delivery system has enhanced efficacy in targeted drug delivery and release, providing optimal therapeutic outcomes.

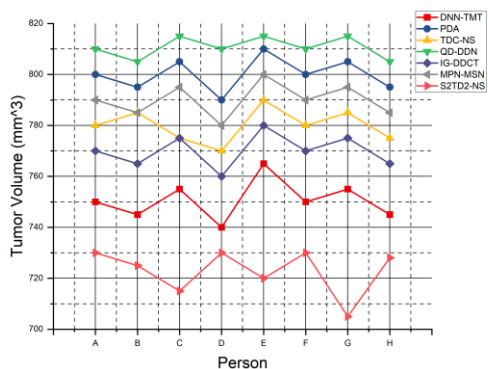


Fig.5. Tumor volume analysis.

The tumor volume data for several people are reported in Figure 5. The mean values for each approach are as follows: DNN-TMT (750.63 mm³), PDA (800 mm³), TDC-NS (780 mm³), QD-DDN (810.63 mm³), IG-DDCT (770 mm³), MPN-MSN (790 mm³), and S2TD2-NS (722.88 mm³). The S2TD2-NS intervention exhibits the most substantial decrease in tumor volume, averaging 722.88 mm³. This observation suggests that it has a heightened capacity to impede the proliferation of tumors, presenting a hopeful avenue for cancer treatment.

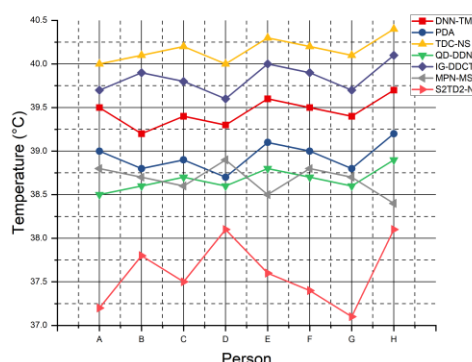


Fig.6. Temperature analysis.

Figure 6 presents the temperature findings for several persons. The mean values for each approach are as follows: DNN-TMT (39.45°C), PDA (38.94°C), TDC-NS (40.16°C), QD-DDN (38.68°C), IG-DDCT (39.84°C), MPN-MSN (38.68°C), and S2TD2-NS (37.6°C). The S2TD2-NS method consistently yields the lowest temperature, with an average of 37.6°C. This observation suggests there is a possibility for the targeted administration of drugs in a specific area while minimizing heat production. This, in turn, decreases the likelihood of causing harm to nearby healthy tissues due to heat.

The S2TD2-NS exhibits notable outcomes, with mean values of 89.33% for encapsulation efficiency, 1.33 for fluorescence intensity ratio, 722.88 mm³ for tumor volume, and 37.6°C for temperature. The results above underscore the efficacy of S2TD2-NS in augmenting drug encapsulation, facilitating targeted drug release, reducing tumor volume, and decreasing heat production. This strategy has considerable potential for the treatment of cancer.

CONCLUSION AND FUTURE SCOPE

To effectively navigate the intricacies of tumor therapy, it is essential to use novel methodologies for medication administration. A TME presents considerable obstacles due to its ability to impede medication penetration and provide an unfavorable setting for therapeutic interventions. The attainment of optimum treatment results heavily relies on the efficacy of medication delivery. It is essential to prime the TME to optimize medication penetration, augmenting therapeutic interventions' effectiveness. Using size-tunable drug delivery NSs has emerged as a viable approach to address these difficulties. The present study introduces the Smart Size-Tunable Drug Delivery Nanosystems (S2TD2-NS) as a potential solution for enhancing drug encapsulation efficiency using (R)-(+)- α -LA. The findings show promise, as indicated by an average encapsulation effectiveness of 89.33%, a fluorescence intensity ratio of 1.33, a significant decrease in tumor volume to 722.88 mm³, and limited heat production at 37.6°C.

Nevertheless, there are still obstacles to overcome, such as concerns over the stability and scalability of S2TD2-NS. Furthermore, the prospects of this methodology include further improvement, assessment of its long-term effectiveness, and potential for clinical use. S2TD2-NS presents a promising avenue for better drug administration and heightened therapeutic efficacy in pursuing more efficacious cancer therapy. As the constraints of current methodologies are acknowledged and the suggested technique is further developed, the forthcoming prospects include enhanced efficacy in cancer therapies, elevated patient care standards, and augmented patient survival rates.

REFERENCES

1. Nazemi Rafie A, Dalvandi M, Jalili H, Kamali A. Overall survival for the patients with central nervous system (CNS) tumors during 9 years follow-up in Markazi province of Iran. *Onkologia I Radioterapia*. 2020;1(50):146-150. [Google Scholar](#) | [Crossref](#)
2. Catrina SB, Zheng X. Hypoxia and hypoxia-inducible factors in diabetes and its complications. *Diabetologia*. 2021;64:709-716. [Google Scholar](#) | [Crossref](#)
3. Dewi A, Upara C, Krongbamee T, Louwakul P, Srisuwan T, Khemaleelakul S. Optimal antimicrobial concentration of mixed antibiotic pastes in eliminating

- Enterococcus faecalis from root dentin. *Aust Endod J*. 2021;47(2):273-280. [Google Scholar](#) | [Crossref](#)
4. Dai C, Tang Z, Li X, Chen T. High-pressure homogenization and tailoring of size-tunable Ganoderma lucidum spore oil nanosystem for enhanced anticancer therapy. *Chem Eng J*. 2021;406:127125. [Google Scholar](#) | [Crossref](#)
5. Kheraldine H, Rachid O, Habib AM, Al Moustafa AE, Benter IF, Akhtar S. Emerging innate biological properties of nano-drug delivery systems: A focus on PAMAM dendrimers and their clinical potential. *Adv Drug Deliv Rev*. 2021;178:113908. [Google Scholar](#) | [Crossref](#)
6. Luan L, Tang B, Liu Y, Xu W, Liu Y, Wang A, Niu Y. Direct synthesis of sulfur-decorating PAMAM dendrimer/mesoporous silica for enhanced Hg (II) and Cd (II) adsorption. *Langmuir*. 2022;38(2):698-710. [Google Scholar](#) | [Crossref](#)
7. Smith OE, Waters LJ, Small W, Mellor S. CMC determination using isothermal titration calorimetry for five industrially significant non-ionic surfactants. *Colloids Surf B Biointerfaces*. 2022;211:112320. [Google Scholar](#) | [Crossref](#)
8. Cruz Barrios E, Annunziata O. Determination of critical micelle concentration from the diffusion-driven dilution of micellar aqueous mixtures. *Langmuir*. 2021;37(8):2855-2862. [Google Scholar](#) | [Crossref](#)
9. D'Amico RS, Aghi MK, Vogelbaum MA, Bruce JN. Convection-enhanced drug delivery for glioblastoma: A review. *J Neurooncol*. 2021;151:415-427. [Google Scholar](#) | [Crossref](#)
10. Large DE, Abdelmessih RG, Fink EA, Auguste DT. Liposome composition in drug delivery design, synthesis, characterization, and clinical application. *Adv Drug Deliv Rev*. 2021;176:113851. [Google Scholar](#) | [Crossref](#)
11. Yang B, Meng F, Zhang J, Chen K, Meng S, Cai K, et al. Engineered drug delivery nanosystems for tumor microenvironment normalization therapy. *Nano Today*. 2023;49:101766. [Google Scholar](#) | [Crossref](#)
12. Ju Y, Wang Z, Ali Z, Zhang H, Wang Y, Xu N, et al. A pH-responsive biomimetic drug delivery nanosystem for targeted chemo-photothermal therapy of tumors. *Nano Res*. 2022;15(5):4274-4284. [Google Scholar](#) | [Crossref](#)
13. Chen L, Hong W, Duan S, Li Y, Wang J, Zhu J. Graphene quantum dots mediated magnetic chitosan drug delivery nanosystems for targeting synergistic photothermal-chemotherapy of hepatocellular carcinoma. *Cancer Biol Ther*. 2022;23(1):281-293. [Google Scholar](#) | [Crossref](#)
14. Wu H, Wei M, Xu Y, Li Y, Zhai X, Su P, et al. PDA-based drug delivery nanosystems: a potential approach for glioma treatment. *Int J Nanomed*. 2022;3751-3775. [Google Scholar](#) | [Crossref](#)
15. Behrooz AB, Vazifehmand R, Tajudin AA, Masarudin MJ, Sekawi Z, Masomian M, Syahir A. Tailoring drug co-delivery nanosystem for mitigating U-87 stem cells drug resistance. *Drug Deliv Transl Res*. 2022;12(5):1253-1269. [Google Scholar](#) | [Crossref](#)
16. Ruzycka-Ayoush M, Kowalik P, Kowalczyk A, Bujak P, Nowicka AM, Wojewodzka M, et al. Quantum dots as targeted doxorubicin drug delivery nanosystems in human lung cancer cells. *Cancer Nanotechnol*. 2021;12:1-27. [Google Scholar](#) | [Crossref](#)
17. Priestler MI, Ten Hagen TL. Image-guided drug delivery in nanosystem-based cancer therapies. *Adv Drug Deliv Rev*. 2022;114621. [Google Scholar](#) | [Crossref](#)
18. Gao Y, Yang SC, Zhu MH, Zhu XD, Luan X, Liu XL, et al. Metal phenolic network-integrated multistage nanosystem for enhanced drug delivery to solid tumors. *Small*. 2021;17(29):2100789. [Google Scholar](#) | [Crossref](#)